

AD-A248 882



DOCUMENTATION PAGE

Form Approved
OMB No. 0704-0186

1a. REPORT SECURITY CLASSIFICATION			1b. RESTRICTIVE MARKINGS			
2a. SECURITY CLASSIFICATION AUTHORITY			3. DISTRIBUTION/AVAILABILITY OF REPORT This document has been approved for public release and sale; its distribution is unlimited.			
2b. DECLASSIFICATION/DOWNGRADING SCHEDULE						
4. PERFORMING ORGANIZATION REPORT NUMBER(S)			5. MONITORING ORGANIZATION REPORT NUMBER(S) ARO 28436.1-MS-SBI			
6a. NAME OF PERFORMING ORGANIZATION Implant Sciences Corporation		6b. OFFICE SYMBOL (If applicable)		7a. NAME OF MONITORING ORGANIZATION US Army Research Office Material Science Division		
6c. ADDRESS (City, State, and ZIP Code) 107 Audubon Road, 5 Corporate Place Wakefield, MA 01880-1246			7b. ADDRESS (City, State, and ZIP Code) P. O. Box 12211 Research Triangle Park, NC 27709-2211			
8a. NAME OF FUNDING/SPONSORING ORGANIZATION US Army Laboratory Command, Army Research Office		8b. OFFICE SYMBOL (If applicable)		9. PROCUREMENT INSTRUMENT IDENTIFICATION NUMBER DAAL03-91-C-0014		
8c. ADDRESS (City, State, and ZIP Code) P. O. Box 12211 Research Triangle Park, NC 27709-2211			10. SOURCE OF FUNDING NUMBERS			
			PROGRAM ELEMENT NO. SBIR		PROJECT NO.	TASK NO.
			WORK UNIT ACCESSION NO.			
11. TITLE (Include Security Classification) Strongly Adherent Ceramic Surface Layers by Ion Implantation (U)						
12. PERSONAL AUTHOR(S) Stephen N. Bunker						
13a. TYPE OF REPORT Final		13b. TIME COVERED FROM 3/91 TO 9/91		14. DATE OF REPORT (Year, Month, Day) 91-12-15		15. PAGE COUNT
16. SUPPLEMENTARY NOTATION						
17. COSATI CODES			18. SUBJECT TERMS (Continue on reverse if necessary and identify by block number)			
FIELD	GROUP	SUB-GROUP	Coating, ZrO ₂ , Ion Implantation, Adhesion			
19. ABSTRACT (Continue on reverse if necessary and identify by block number) See attached page						
<div style="text-align: right;"> DTIC ELECTE APR 20 1992 </div> <div style="text-align: center;"> 92-09937 </div> <div style="text-align: center;"> 92 4 17 009 </div>						
20. DISTRIBUTION/AVAILABILITY OF ABSTRACT <input checked="" type="checkbox"/> UNCLASSIFIED/UNLIMITED <input type="checkbox"/> SAME AS RPT. <input type="checkbox"/> DTIC USERS			21. ABSTRACT SECURITY CLASSIFICATION U			
22a. NAME OF RESPONSIBLE INDIVIDUAL Dr. Anthony J. Armini			22b. TELEPHONE (Include Area Code) (617) 246-0700		22c. OFFICE SYMBOL	

Summary Abstract

Many applications exist for specialized coatings which must never debond during their working life. Ceramic coatings on metals are particularly important for this special category, but the dissimilar properties of the two types of materials make most existing coating techniques unacceptable. Ion implantation is well-known to produce totally adherent depositions of atoms, because the high energy of the ion beam causes the atoms to come to rest inside the target material rather than lay upon it. Thus, there is no discrete surface for debonding. Unfortunately, it has rarely been possible to accumulate enough ion implanted atoms in one place to form a pure layer because the sputtering coefficient is usually greater than unity.

This research has developed a technique of co-depositing a sacrificial layer together with ion implantation in order to create an effective sputtering coefficient of zero. Implanted atoms can accumulate to arbitrarily thick layers which are physically merged to the substrate. A demonstration of the general techniques has been performed using Zirconium as the ion. The Zirconium has been converted to zirconia, ZrO_2 , by reaction with a low pressure background of oxygen in the process chamber.

The zirconia coatings show extreme adhesion using scratch testing and by repeated $600^\circ C$ fast thermal cycling. Many observed properties as well as Auger analysis confirm they are ZrO_2 . Coatings were tested as a base layer for conventional ZrO_2 coating technologies, and deposition on both flat and curved surfaces was demonstrated.

While a number of important applications have been already identified, initial interest has focussed on moving components used in military diesel engines produced by Cummins Engine Company. The ability of the coating to maintain accurate tolerances and to provide an environmental barrier over a wide range of temperatures will be essential for improving fuel efficiency and decreasing maintenance down-time.

Accession For	
NTIS CRA&I	<input checked="" type="checkbox"/>
DTIC TAB	<input type="checkbox"/>
Unannounced	<input type="checkbox"/>
Justification	
By <i>per form 50</i>	
Distribution /	
Availability Codes	
Dist	Avail and/or Special
A-1	



FINAL REPORT FOR
STRONGLY ADHERENT CERAMIC SURFACE LAYERS
BY ION IMPLANTATION

Contract: DAAL03-91-C-0014

Submitted to:

U. S. Army Research Office
P. O. Box 12211
Research Triangle Park, NC 27709-2212
Attn: Mr. Richard O. Ulsh

Submitted by:

Implant Sciences Corporation
35 Cherry Hill Drive
Danvers, MA 01923

I. INTRODUCTION TO THE PROBLEM

Many applications exist that call for a coating with unusually reliable adhesion to the substrate. Ion implantation has long been known for the remarkable adhesion of the implanted atoms, but it has been thought of as incapable of providing the thickness characteristic of a coating process. This final report describes a new technique using ion implantation which has succeeded in making thick layers of zirconia, ZrO_2 , on arbitrary substrates. Coatings were produced that emphasized several specific commercial applications.

It is widely recognized that perhaps the only deposition technique for absolutely guaranteeing adhesion is that of ion implantation. This results from two key effects. First, atoms are added sub-surface rather than deposited on the surface, and second, there is no abrupt interface between the dissimilar materials. The former effect largely ensures a deposit free from ambient impurities and the latter creates a graded interface ideal for merging mismatched materials.

There is a second problem inherent with coating by ion implantation. Only atoms are implanted, not molecules, and most desirable refractory materials are compounds. However, it is possible to use reactive ion implantation in the case of some transition metal oxides, such as zirconium.

The commercial use of ion implantation coatings is a specialized market that would be applicable when conventional coating processes are deficient in one or another property. Unquestionably, ordinary physical vapor deposition (PVD) techniques, such as evaporation and sputtering, as well as chemical and electrochemical coatings are well developed and less expensive. A new deposition method, such as described in this report, must initially service niche applications that requires higher performance. Several such applications, both of interest to the Army and the commercial sector, have been identified.

APPLICATIONS

We have concentrated on zirconia, ZrO_2 , as the coating of initial interest even though our technique is general and can apply to a broad variety of materials. ZrO_2 is used in several applications that could benefit from our approach.

1. Diesel Engine Components

Two classes of ZrO_2 coatings are used in diesel engines. The first is the thick thermal barrier coating which is normally made from a plasma sprayed mixture of zirconia and yttrium. The coating thickness is on the order of several thousandths of an inch thick, which is much greater than can be made economically by ion implantation. Alone, without a PVD assist, our

process is limited to the 1 micron regime. It is believed that we could benefit thermal barrier coatings by either preparing an adherent transition layer in the substrate, or by co-evaporating Zirconium to build up thickness. Only the first approach was tested in Phase I.

The second class of ZrO_2 coating in engines is as an electrically insulating protective coating on moving parts in corrosive environments. Cummins Engine Co. is interested in applying the technique to the plungers in the fuel injector system. A motion of about a millimeter occurs regularly, and close tolerances are essential. The insulating coating isolates the plunger for the position monitoring circuitry. Plasma sprayed ZrO_2 coatings were tested and performed well until the inevitable catastrophic failure.

2. Orthopaedic Devices

This is probably one of the more important potential applications. ZrO_2 has already been demonstrated to be biocompatible, and Richards Medical Co. is selling an all- ZrO_2 ball used in a replacement hip joint. The material has been shown to release very few metal ions into the body, it exhibits very low friction onto the ultra high molecular weight polyethylene (UHMWPE) mating cap, and it causes the least production of particle debris from the polyethylene. These three factors are significant, because wear of the polyethylene is the key limiting factor in determining replacement joint life.

Hip balls can be made from pure ZrO_2 because the engineering design of the human body puts the balls into compression, where ceramics are predictably strong. However, the other joints, such as knees, elbows, ankles, or fingers, alternate between tension and compression. Bulk ZrO_2 cannot be used in tension, and the only solution is a durable ZrO_2 coating on a metal base, an ideal application for our technology.

Today's technology produces artificial joints that normally last 10 years. For the elderly this is acceptable, but for the young, including battlefield casualties, the regular repetition of massive surgery is a serious problem both for insurance companies and the Veteran's Administration. Such procedures are very costly, and the long term liability and expense for either a young veteran or civilian is predictably massive. Anything that extends the lifetime of orthopaedic joint replacements will yield a dramatic cost savings for both the public and the government.

3. Adherent Coatings for Industry

This is a less well-defined market which consists of many smaller applications. One use would be as a low friction protective coating for magnetic tape heads. ZrO_2 has already been shown to work well in this application, but the PVD coating fails catastrophically.

TECHNOLOGY INNOVATION

Making an adherent coating of ZrO_2 by ion implantation requires arbitrary concentrations of Zirconia atoms to be added into a surface. A well-known rule, however, states that the maximum atomic percent of ion implantation atoms is given by:

$$\text{Limiting Atomic Percent} = 1/S * 100\%$$

Where S is the sputtering coefficient. The 1/S rule states that at a certain accumulated dose, the removal rate of surface atoms by sputtering will equal the addition rate of implanted atoms. Thus, a saturation limit exists for the concentration of added atoms. It is circumventing this natural limit that we have addressed in our research.

If the sputter coefficient could be reduced to zero, of course, the rule would not apply, and this is how conventional physical vapor deposition coatings can be added to build up thickness. The key technique, then, is to simulate a zero sputter coefficient by continuously applying a sacrificial PVD coating at the same rate as the sputter erosion.

There are several unusual consequences of a zero sputter coefficient during high energy ion implantation. First, atoms can be added indefinitely, building up layers to arbitrary thickness. Second, growth takes place from the inside-out, rather than on the surface. Problems of contamination inclusion from the environment are automatically avoided. Third, a gradual transition from substrate atoms to added atoms occurs as the material swells from within and becomes more enriched in added atoms.

The sacrificial coating may be any solid species, and for our research Silver was used. Silver was selected because it does not oxidize easily, it is distinct from Zirconium and can be independently identified, and because it can easily be evaporated using simple equipment. Zirconium is more refractory, is oxidation sensitive, and for analysis purposes, it would be impossible to differentiate between implanted versus coated atoms.

For long term commercial purposes, in contrast to this research program, the use of an atomic species identical to the metal being implanted is important. In a manner similar to ion beam assisted deposition (IBAD), coatings could be grown more rapidly by incorporating the sacrificial atoms into the coating. This would be suitable in the thickness range from 1 micron to perhaps 10 to 50 microns. However, no research was done on this technique during Phase I, because the emphasis was on the initial demonstration of the zero sputtering coefficient effect.

The purpose of this research is actually to make ZrO_2 , not Zr. The oxygen could have been added in 2 ways, and fortunately both methods were immediately successful. This simplest approach is to use reactive ion implantation in which the process chamber is backfilled to a low pressure of oxygen. In practice an air backfill was also found to work. The more difficult method is to ion implant the oxygen as well as the Zirconium. Test runs were performed early in the program to demonstrate the effect, and colorful optical interference layers of transparent

ZrO₂ were readily fabricated. However, the process is much more costly than the reactive approach. A detailed description of how stoichiometric layers of ZrO₂ can be produced using oxygen ion implantation will be given in section 2 when the test is discussed.

II. RESEARCH PROGRAM

The technical objectives of the research program are reproduced below from the Phase I proposal. All of these objectives were met successfully.

1. Demonstrated that Zirconium and Oxygen ion implantation makes self-limiting stoichiometric ZrO₂.
2. Demonstrate that a zero sputtering coefficient can be obtained for Zr metal implantation.
3. Demonstrate that a ZrO₂ layer can be grown by surface modification on an arbitrary substrate
4. Characterize the films created in each of the above steps.

In addition, other related research was conducted because of the early success in completing these objectives. These tests included the following:

1. Real commercial parts were coated for Cummins Engine Company.
2. Coating of a cylindrical surface was demonstrated.
3. The ion implanted surface was tested as a interface for conventional PVD coating.
4. Complex surfaces were coated.
5. A variety of substrate materials was coated(M50, D2, stainless steel, gold, aluminum, cobalt chrome alloy, silicon)

2.1 ZrO₂ by Ion Implantation of Oxygen (Technical Objective #1)

The reactive ion implantation process discovered later in the research made this technical objective unnecessary. The work described in this subsection was performed early in the program and is included here for completeness.

Normally, when ions are implanted into metal substrates, a spacial distribution of atoms with depth is produced which has the shape of a skewed Gaussian. The depth of the center of the Gaussian is at or near the "range", and the width of the Gaussian is related to a parameter called the "skewness". These parameters can be predicted, and Implant Sciences sells a software program to do this. However, when Oxygen is implanted into some metals at sufficiently high

dose, the depth distribution of atoms becomes modified and broadens. A peak concentration of Oxygen corresponding to the natural stoichiometry of this metal oxide is observed.

The effect is caused by the very high radiation assisted diffusion constant for Oxygen in the oxide, and has been observed in many metals. Well known examples include Be, Al, Si, Ti, and now Zr. As Oxygen is added into the metal, the normal Gaussian distribution occurs until stoichiometry for the oxide is reached at some depth. Then, if another Oxygen atom is added, it diffuses quickly out of the oxide in the direction of maximum radiation-induced defects, that is, toward the outside surface. As soon as the diffusing atom is outside of the oxide layer, it reacts with the first metal atom it encounters and stops diffusing. Thus, a buried oxide layer gradually grows outward toward the surface. Oxygen atoms implanted in depth migrate to the edge of the buried layer until the layer thickness is enough to reach the surface. At that time the layer becomes visible because the quality of the oxide is adequate to be optically transparent, thus causing multiple light reflections. The optical interference is observed as a colorful iridescence whose hue is related to the thickness of the oxide. All colors from red to blue can be created.

The required dose of oxygen, D , is related to the range, R , of the ions. It is given by

$$D \text{ (atoms/cm}^2\text{)} = \frac{2 * \text{Rho} * N_{Av} * R \times 10^{-8}}{M}$$

where M and Rho are the atomic weight and density of Zirconium, and N_{Av} is Avogadro's number, 6.023×10^{23} atoms/mole. R is in Angstroms. A typical value of D for 150keV oxygen ions is 1.7×10^{18} atoms/cm².

Sample plates of zirconium, 2 inches square, were bombarded with Oxygen ions at 100keV at doses of 1×10^{18} ions/cm² (vacuum ambient at 3×10^{-6} Torr or better) and 5×10^{17} ions/cm² (O_2 or H_2O at 2 to 5×10^{-5} Torr). The sample implanted at 1×10^{18} /cm² should have received enough oxygen atoms to convert a zone about 750 Angstroms thick into pure ZrO_2 . The dose at 5×10^{17} /cm² should have been insufficient to make ZrO_2 without an assist from the ambient gases.

Figure 2 shows a prediction for the expected profiles based on our Profile Code™. The calculation has been performed using a highdose model in which the change in composition of the substrate is computed and the range, sputtering, etc. are modified continuously during the buildup of the profile. The specific model used assumes that oxygen diffuses rapidly in ZrO_2 , thus allowing the excess oxygen to diffuse toward the edges of the growing buried layer. Since ion enhanced diffusion tends to increase diffusion speed towards the outside surface, most Oxygen atoms move in this direction, thus producing the asymmetric shape for the profile at 1×10^{18} /cm².

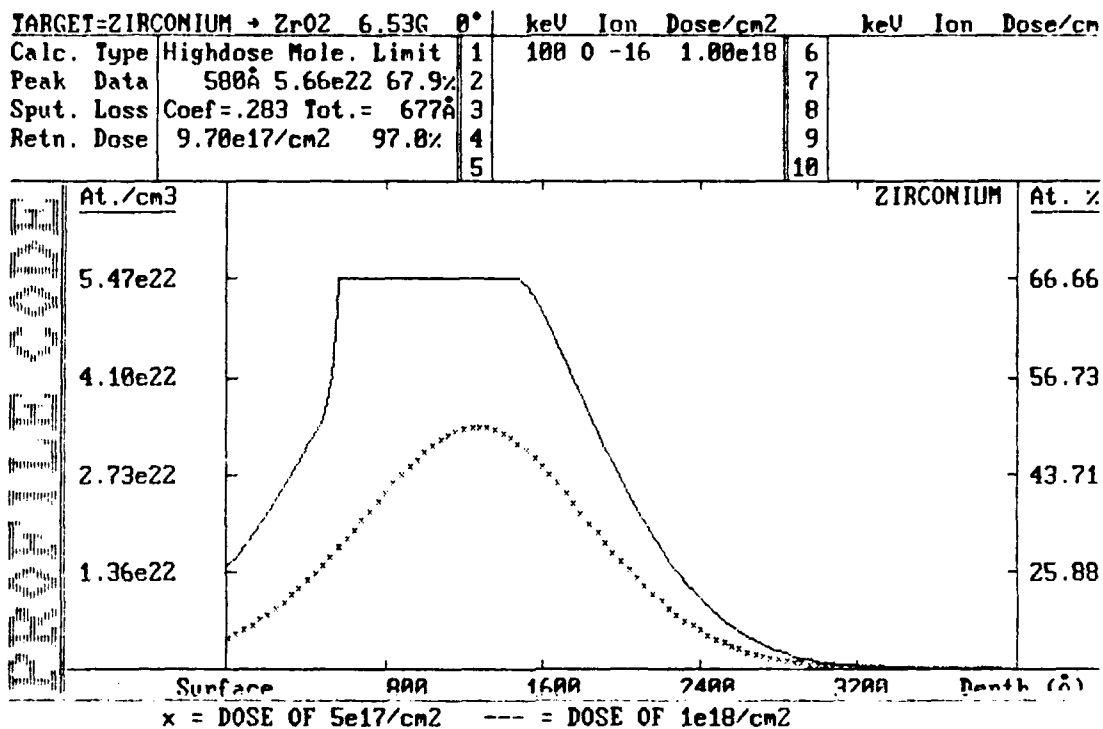


Figure 2. Profile Code Prediction of the Oxygen Distribution.

Figures 3 and 4 show Auger Electron Spectroscopy (AES) depth profiles for the $1 \times 10^{18}/\text{cm}^2$ and $5 \times 10^{17}/\text{cm}^2$ samples, respectively. The surface of the samples was too rough for independent verification of the depth scale. Based on fitting to the Profile Code depth scale, it appears that an approximate calibration would be 75.8 Angstroms per minute of sputtering.

The remarkable feature of these Auger profiles is the perfect stoichiometry of oxide all the way to the surface. The two figures differ only in the deep features above the 15 minute mark, and that can be attributed to the differences in the right-hand edge of the predicted as-implanted profiles. Oxygen ion implantation into Zr appears to gather oxygen from the chamber very efficiently, because the near surface area has been filled with stoichiometric oxide, and the integral of the total oxygen present well exceeds that which was implanted.

Using the sputter calibration given above, the deep Auger data above the 20 minute mark fairly closely matches the shape predicted, thus suggesting the ion enhanced diffusion is only important nearer the surface. Both implanted samples showed the visible interference color fringes characteristic of transparent thin films, but the low dose sample was less saturated in color, consistent with the optical effect of a less sharply defined back surface. Since the high dose sample was implanted first and the vacuum was good for this run, the complete filling-in of the profile near the surface was particularly surprising. The addition of either O_2 or H_2O did not appear to significantly change the effect.

There were several other general observations about implanted layers. First, adhesion was excellent, as expected for ion implantation. Second, unlike Titanium substrates, the ZrO_2

layer is not affected by excess oxygen buildup over stoichiometry. This implies that Oxygen diffuses very rapidly in ZrO_2 , and can escape to the vacuum, if needed, when full stoichiometry is attained. Third, the rapid diffusion of ambient Oxygen implies that ion enhanced diffusion is a particularly strong effect in this system, and thus a wide range of ion species can be implanted without profoundly affecting the diffusion rate.

In summary Zirconium appears to oxidize very readily to form thin films of ZrO_2 . High energy Oxygen implantation appears to draw further oxygen efficiently from the background gases of the implant vacuum chamber. Because of these observations, there was early confidence that the reactive ion implantation method would be successful.

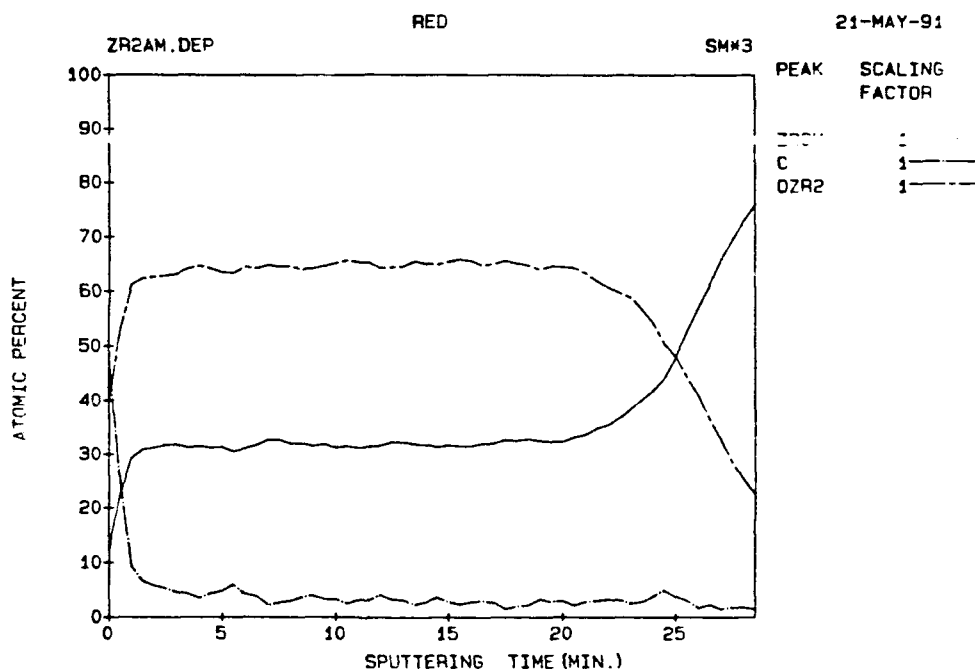


Figure 3. Auger Data for Dose of $1 \times 10^{18} \text{ O}^+/\text{cm}^2$ into Zirconium. Vacuum was $3 \times 10^{-3} \text{ Torr}$ with no added gases.

2.2 Preliminary Proof-of-Principle (Technical Objective #2)

Our technique for ion implantation coating depends on deposition of a sacrificial coating at a controlled rate to balance the surface sputter loss. Fortunately, there is some latitude in rates, and a precise balance is not essential, just more efficient.

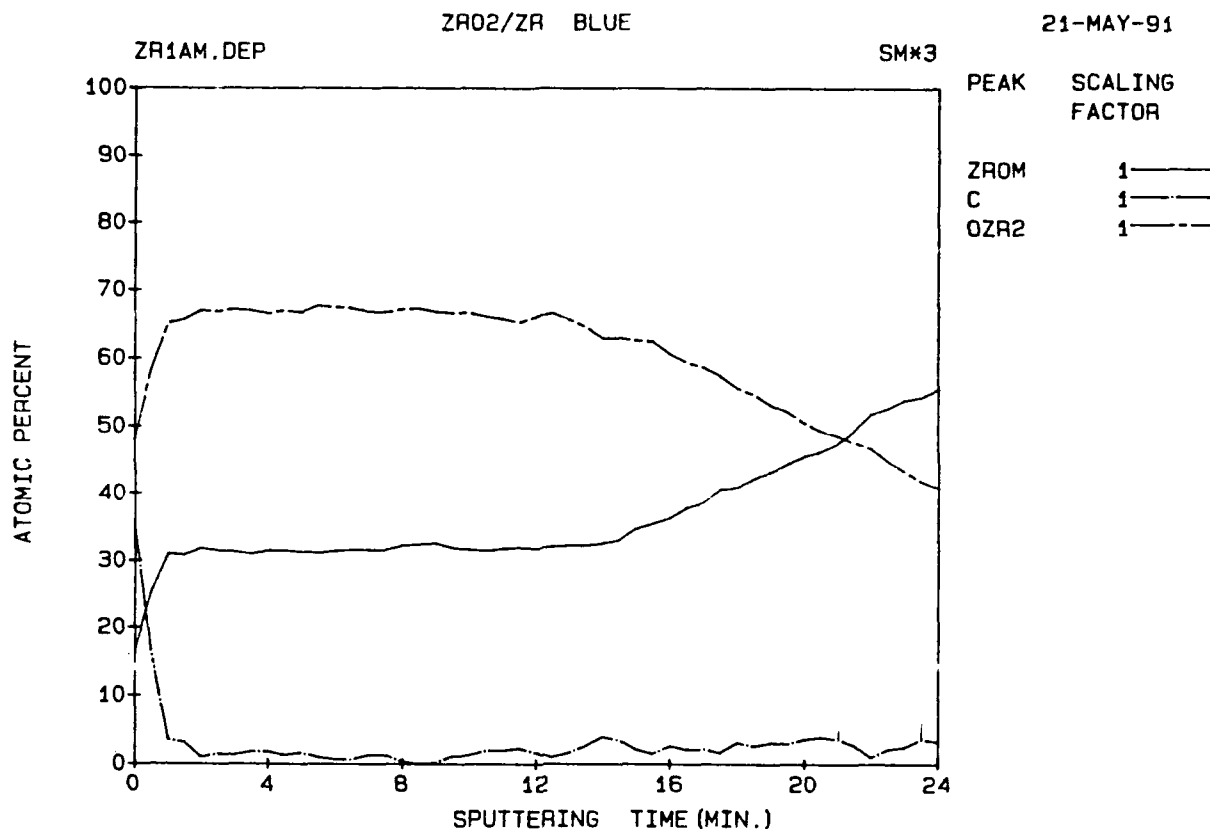


Figure 4. Auger Data for Dose of $5 \times 10^{17} \text{ O}^+/\text{cm}^2$ into Zirconium. Vacuum was 4×10^{-5} Torr with H_2O vapor added

Simultaneously coating and ion implanting yields a continuum of coating types depending on the relative fluxes, and exactly balancing sputter loss by coating is just a special case of a broader series of effects. If the sacrificial coating rate approaches zero, one has conventional ion implantation. As the rate increases, the concentration of retained ion species also increases, but all coating atoms are removed. When the effective sputtering coefficient becomes less than one, the ions implanted can accumulate to form a slowly thickening layer, although some implanted ions are still being sputtered away. The efficiency of this process peaks at a sputtering coefficient of zero, when all implanted ions are retained. For still higher sacrificial coating fluxes, the coating species becomes retained as a percentage of the growing surface along with the accumulating ions. This last extreme case is commonly referred to as Ion Beam Assisted Deposition. Our research in Phase I has concentrated on the middle region where highly enriched layers can be created solely from the ion beam species.

The sacrificial coating can be created by any physical vapor deposition (PVD) process. Initially, we tested sputtering, sharing the ion beam between the test sample and a sputter target, as shown in Figure 5. This scheme is simple, requiring only an ion implanter and a controlled deflector. The duty factor for relative time on the sputter target verses the main target was trimmed to yield a small net gain in main target thickness.

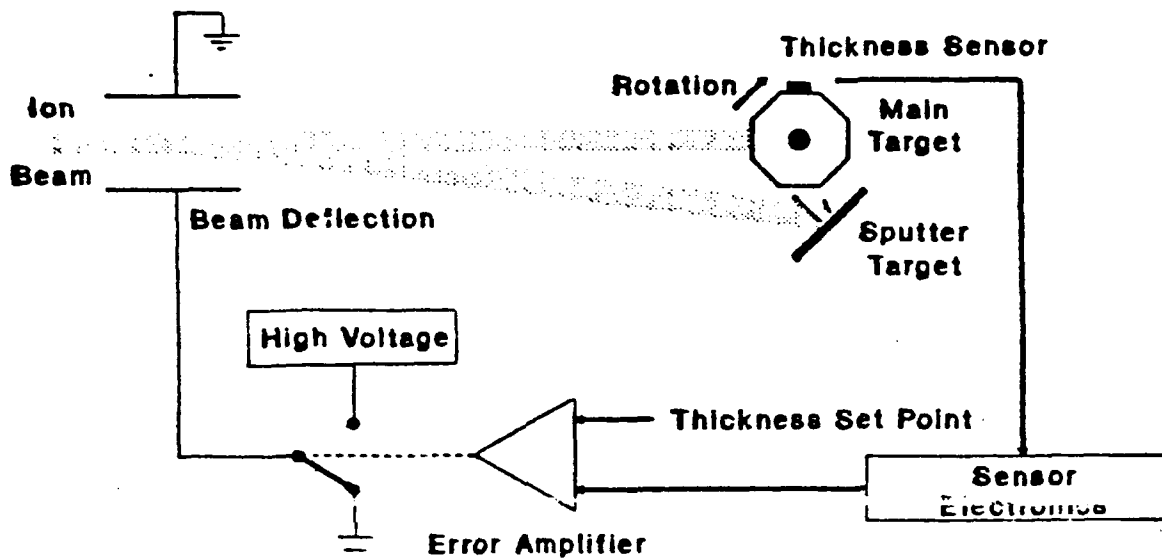


Figure 5. System For Ion Implantation of Zirconium with Concurrent Deposit of a Sacrificial Coating. The Ion Beam is Alternately Aimed at the Sputter Target and the Bearing Steel Target.

A commercial quartz crystal thickness sensor was acquired from SYCOM for use on this program. In preliminary trials before the SYCOM unit was delivered, masked Silicon wafers were used as test substrates. The thickness change across the mask edge on the wafer was used as an indicator of the balance in sputter and deposition rates. A Tencor Alpha Step profilometer measured these step heights.

As the dwell time on the sputter target was increased, the step eventually became positive at a duty factor of 15:1. This means that the beam needed to be on the sputter target 15 times longer than the wafer, a very inefficient situation for the Zirconium ion beam. For this reason we choose to investigate evaporation to achieve the sacrificial coating, because this approach is more compatible with commercial requirements, and because an evaporator could be used for thickening the coating.

In summary the results of this test showed the following:

1. Sputtering to produce a sacrificial coating is feasible but impractical.

2. Control of the coating rate can make the effective sputtering coefficient become zero.

2.3 Evaporator Design and Fabrication

An evaporator is the obvious method for producing the sacrificial coating. The most versatile evaporator is the electron-beam type, but the resources were not available to purchase, install, and debug such a system during this program. Instead, a simple resistance-heated boat system was constructed and mounted in the ion implanter end station. Figure 6 shows the configuration of this system, which consists of 2 power busses, a connecting tantalum foil boat, a cooled shield, and a shutter. The cooled shield served the dual purpose of minimizing radiated heat to the rest of the chamber and providing an electrical shield to avoid erroneous Faraday cup readings. The end station system in use requires the entire vacuum chamber to collect ion beam charge for current integration. Any scattered electrons attracted to the evaporator electrical connections would be lost without the shield.

With experience it was found that the quartz crystal oscillator did not operate reliably when directly exposed to the ion beam. Although electrical separation of earth and Faraday grounds was maintained with an isolation transformer, it was observed that an unusually long time constant in reaching stabilization of the reading was required. Whenever any electrical parameter was changed, such as power to the evaporator boat or ion beam current, the displayed evaporation rate would abruptly shift and then slowly recover. At long as the system was electrically stable, the thickness gauge appeared reliable. This technical problem was resolved by placing the gauge outside of the ion beam and only measuring the evaporation rate. This was matched to a theoretical prediction of the required rate at a given beam current density. The expression for evaporation rate E in Angstroms per second is given by

$$E = \frac{M \cdot S \cdot I}{P \cdot N_{av} \cdot A \cdot 1.6 \times 10^{-27}}$$

Where M = Molecular weight of evaporant

S = Sputtering coefficient of ion on evaporant

I = Ion current in Amperes

P = Density of evaporant

N_{av} = Avogadro's number

A = Area of ion beam in cm^2

Typically, it was found that low evaporation rates between 0.5 and 1.5 Angstroms per second were required.

The choice of evaporant was more difficult. A substance was needed that evaporated steadily and was distinct from the Zirconium ion beam in order to facilitate later analysis. Both Aluminum and Silver were tested. It was observed that Silver, which was neither chemically reactive to background Oxygen in the chamber nor alloyed with the boat, was the best choice,

and all subsequent tests were made with this material. Although Silver is probably impractical from a commercial viewpoint, it was ideal for the research. Subsequent analyses, which will be described later, showed no evidence of entrapped Silver in the ZrO_2 coating except for very thin surface films.

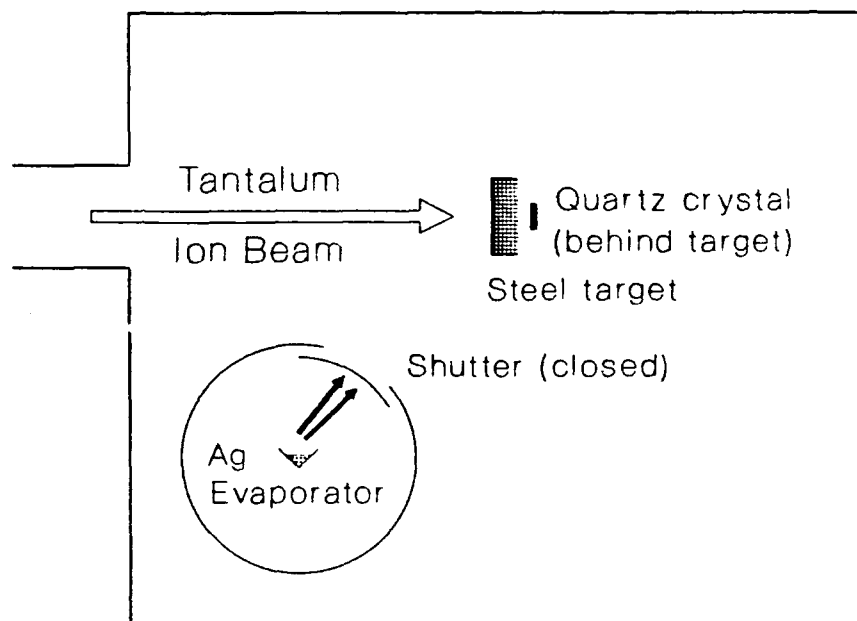


Figure 6. Schematic Layout of the Evaporation System Used to Generate the Sacrificial Coating

2.4 Initial Evaporator Trial Run (Technical Objective #3 and #4)

The first test run had the quartz crystal of the crystal oscillator thickness monitor as the target. Specifically, the target was the gold surface coating which composed the electrical contact on the oscillator.

The crystal was selected because it provided the simplest target which could be monitored precisely during the first trial run of the process. It was not the most favorable of targets, however, because the quartz surface was found to be extremely rough (see Figure 7), thus preventing the use of a surface profilometer to measure thickness changes. As such, the depth scale of the Auger spectroscopy data shown in Figure 8 is uncertain.

The sacrificial evaporant was selected to be Aluminum for the first run because it was

convenient and available. Similarly, the implanted ion was selected to be Titanium rather than Zirconium, because Titanium is chemically similar and a regularly produced species on our equipment. Thus, the first trial run was performed with species that were not the same as those intended for regular processing.

Since the target substrate was largely of quartz, there was concern that excessive beam power and heating might crack the material or distort the thickness reading. Thus, the beam current was restricted to a low dose rate, 10 microamperes/cm², and the beam energy was kept at 35keV. This equals a very moderate 0.35 watts/cm². The risk was that the low beam energy might result in impurities because the titanium was being deposited near the surface. On the other hand, if a titanium layer could be created even at such deliberately slow deposition rates and shallow penetration (100 Angstroms range from 35keV Ti⁺ into gold), then it would be a conclusive demonstration that the technique was feasible.

Figure 8 shows the Auger Spectroscopy data. The depth calibration could not be verified by measuring the sputter pit, as previously explained. The quartz thickness monitor indicated an accumulated layer of 686 Angstroms if the sample were coated with pure titanium (TI), and this is consistent with Figure 8. The figure also shows a variable aluminum (ALL) impurity concentration of about 10-15%, mainly near the gold (AUM) interface. The large roughness of the target surface causes the un-sharp edge for the gold interface. The broadening of the edge due to implantation straggle should only be about 100 Angstroms.

The Titanium content was high and relatively flat. We experienced some initial difficulty in learning how to control the relative rates of sacrificial coating and implant, and this is reflected in the unevenness of the residual Aluminum deposit between 500 and 1000 Angstroms. Later on, stable deposit rates were achieved, and this can be seen in the flatter profile of Aluminum between 0 and 500 Angstroms.

There appears to be little carbon contamination in the growing layer, which is unusual for ion implanted Titanium. Gettering from ambient background CO gas is thought to normally cause a carbon exponential "tail" near the surface. We did observe some Oxygen contamination of the film, but it is not shown in Figure 8 because there was no standard sample available to derive an Auger sensitivity factor. Auger is very sensitive to Oxygen, and without the correct factor, Oxygen will dominate the atomic percent unrealistically. At least some of the Oxygen was shown to be bonded to Aluminum, as shown by the shape of the Auger peak. The presence of Oxygen is not unexpected, considering the length of the run (about 6 hours) and the reactivity of Aluminum.

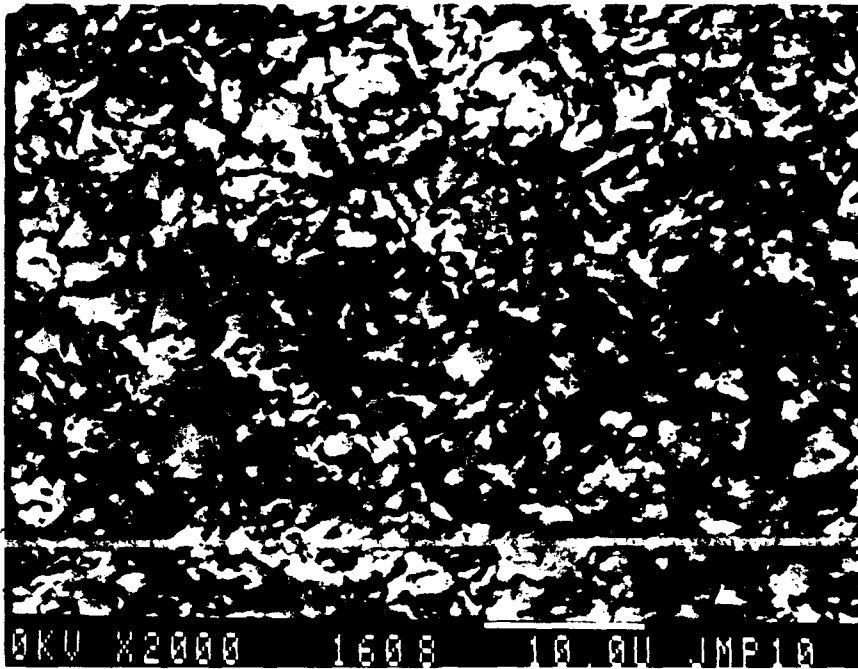


Figure 7. SEM Photo of the Surface of the Gold Coated Quartz Crystal Monitor.

In summary this test run demonstrated the following:

1. An evaporator could be controlled to deposit a sacrificial coating.
2. A nearly pure metal ion implanted coating was formed.
3. Samples with rough surfaces could be coated.
4. Reactive metals may take up Oxygen from the ambient.

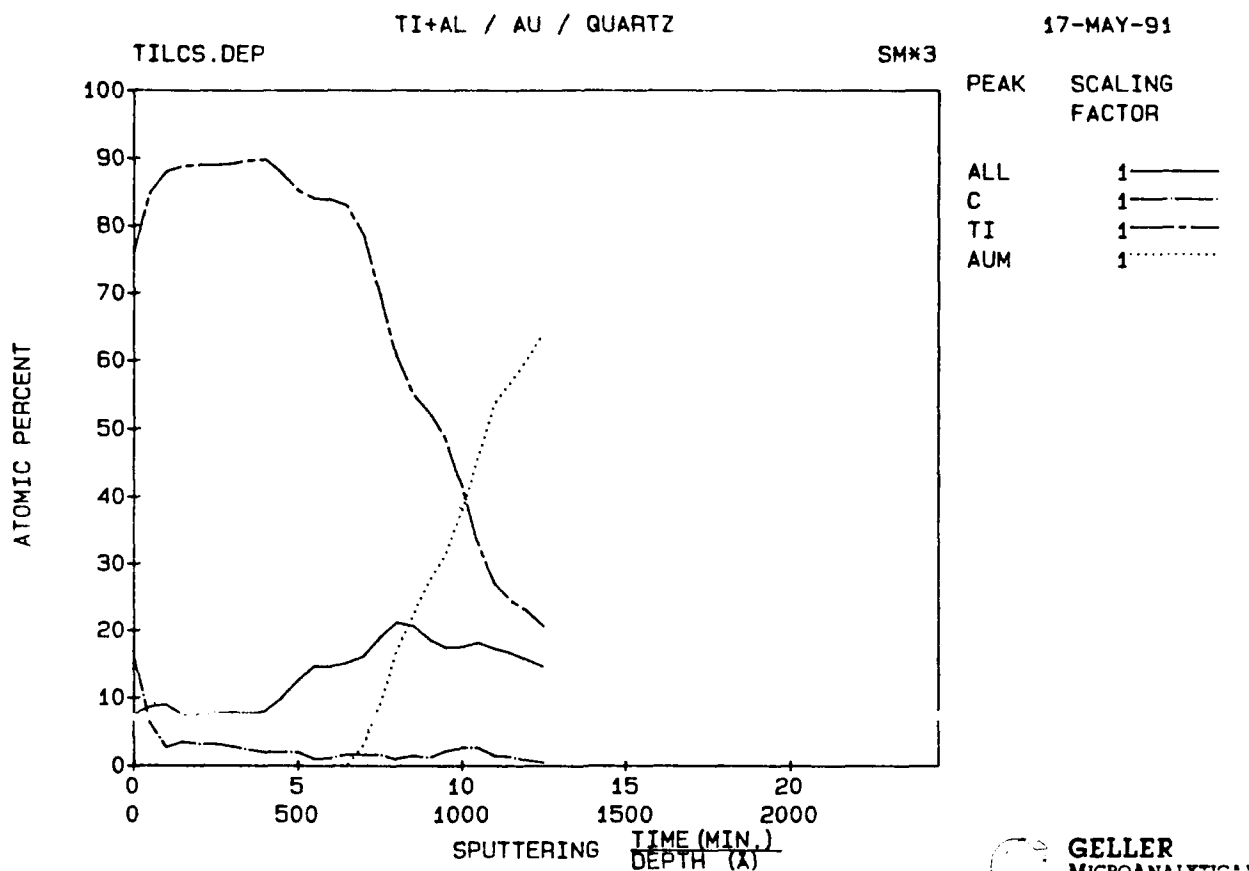


Figure 8. Auger Spectroscopy Data for Titanium Ion Implanted into Gold with Zero Sputtering Coefficient

2.5 Sacrificial Coating Material Selection

It was believed that the best two candidates for the sacrificial coating material would be Zirconium or Yttrium, the former to permit the flexibility of using IBAD and the latter because it is often used to stabilize zirconia coatings. Other candidates included Aluminum and Silver.

Zirconium was never seriously considered during the Phase I effort because an electron beam evaporator would be required. However, in Phase II the choice of Zirconium becomes essential, and appropriate equipment would need to be acquired and installed. Yttrium was attempted but could not be evaporated with our evaporator at a sufficient rate. It was speculated that a refractory oxide was forming on the metal, choking off the evaporant flow even though the tantalum boat had sufficient temperature according to published evaporation data.

It was important during the initial research to use a sacrificial material that was distinct from the constituents of the substrate in order to facilitate identification of any retained evaporant. Until we could get confidence in the process, it was important to learn how much coating contamination to expect. The test of Aluminum was already performed on the gold-coated quartz crystal, but it was observed that Aluminum could not be evaporated for long

enough periods without damage to the boat. Also, it was unclear how much of the retained oxygen was caused by the Aluminum in the quartz crystal sample. Thus, we chose Silver as the primary evaporation material.

Silver can easily be identified in AES analysis. It does not oxidize readily and is compatible with the background Oxygen during reactive ion implantation. The distinctive metallic luster is useful for identifying samples in which the evaporant was emitted at too rapid a rate, thus creating an effective negative sputtering coefficient. When the coefficient is positive, the color fringes of ZrO_2 are obvious, and when it is negative, the fringes are replaced by the characteristic Silver appearance as the silver accumulates.

Tests were done on Silicon, stainless steel, and Aluminum substrates, and Silver performed most reliably, both in maintaining a constant evaporation rate and in reproducibility.

2.6 Reactive Ion Implantation

Reactive ion implantation is simply backfilling the process chamber with Oxygen. The exact pressure was not important, and similar results were obtained over a very wide range of pressures. A pressure of 2×10^{-5} Torr was selected as a compromise to avoid clogging the chamber's cryopumps. No regeneration was required at this level.

The backfill technique is a method that has considerable margin in its application. It worked successfully from the beginning and was used for all subsequent runs. No effort was made to research the lower pressure limit. We tested between 1×10^{-5} to 1×10^{-4} Torr and produced ZrO_2 color fringes in all cases.

2.7 Flat Sample Analysis Specimens

The primary analysis specimen was a highly polished 316SS plate. The established process used 150keV Zr^+ ions, O_2 ambient at 2×10^{-5} Torr, and Silver evaporant. The sample was initially implanted to a dose of about 3×10^{17} Zr^+/cm^2 in order to sputter clean the sample. The expected atomic concentration with depth is shown in Figure 9.

The dose used in cleaning the sample was probably excessive. The intent was to remove both surface contamination and thin the surface skin of iron. It was believed that the iron would have confused the AES analysis results, because it might appear as a low tail of Fe/Cr extending into the ZrO_2 coating. However, this is not really an important consideration.

The flat test sample was ion coated with ZrO_2 for a period determined by the lifetime of the charge of Silver in the evaporator. It was estimated that the accumulated dose of Zr^+ was about $1.3 \times 10^{18}/\text{cm}^2$. In order to coat rapidly the ion beam was not scanned, and thus there existed a spatial variation in dose that matched the variation in current within the beam spot.

This is the reason for the imprecision in estimating the dose.

Many analysis were performed on this test sample, and these are described next.

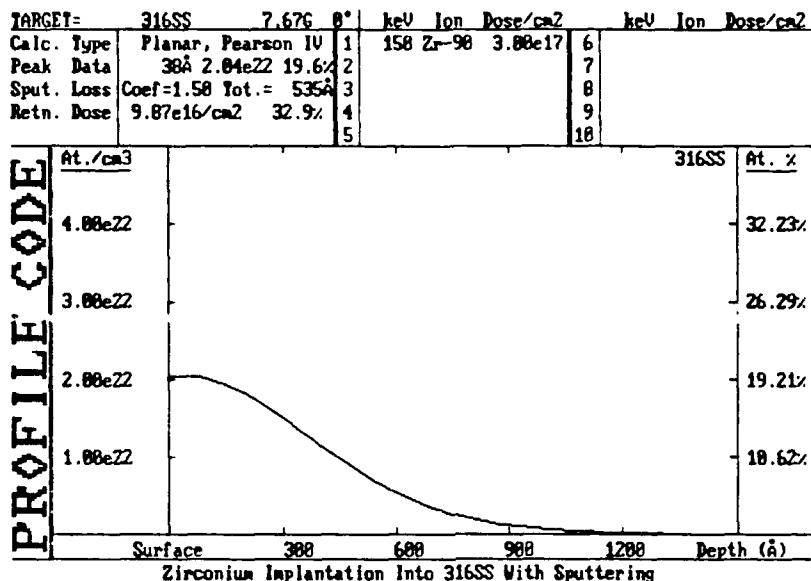


Figure 9. Initial Substrate Preparation Implant Without Sacrificial Coating.

Color

This sample was distinctly gold in color. It could not initially be determined if the color was due to optical interference within a transparent ZrO_2 layer or if it was a discoloration produced by the presence of finely dispersed precipitates of Ag or AgO. It was known from our own experiments that silver ion implanted into glass can produce a similar gold/brown color.

Optical interference colors from a ZrO_2 coating can be predicted if the coating thickness is known. Auger spectroscopy data, which will be discussed later, showed the surface layer to be 2000 Angstroms thick. Using the expression for optical interference maxima,

$$2*n*d=(m+1/2)*L$$

where $n=2.19$ (index of ZrO_2), $d=2000$ Angstroms, L =wavelength, and m = the integer

interference order, one finds that maxima occur at wavelengths of 17200, 5840, and 3440 Angstroms. The first and last wavelengths are in the infrared and ultraviolet with only the maximum at 5840 in the visible. The color yellow occurs between 5700 and 5900 Angstroms. Thus, attributing the color to optical interference of a transparent film is consistent with the observation.

Auger Electron Spectroscopy (AES)

Probably the most useful material analysis data are provided by AES. Surface scans showed the presence of Silver, Carbon, Oxygen, and Zirconium. Together with Iron and Chromium (for the 316 substrate), all of these elements were included in the analysis.

Figure 10 shows typical AES data for the sample. We made other plots from different points on the sample, but these others do not differ significantly. Silver, which would be expected if the proper balance of ion beam dose rate and evaporation rate were not being maintained, is present only near the surface. It begins at about 13 atomic % and drops rapidly. It is speculated that beam irregularities, which caused us to halt the deposition run, are responsible for the surface effect.

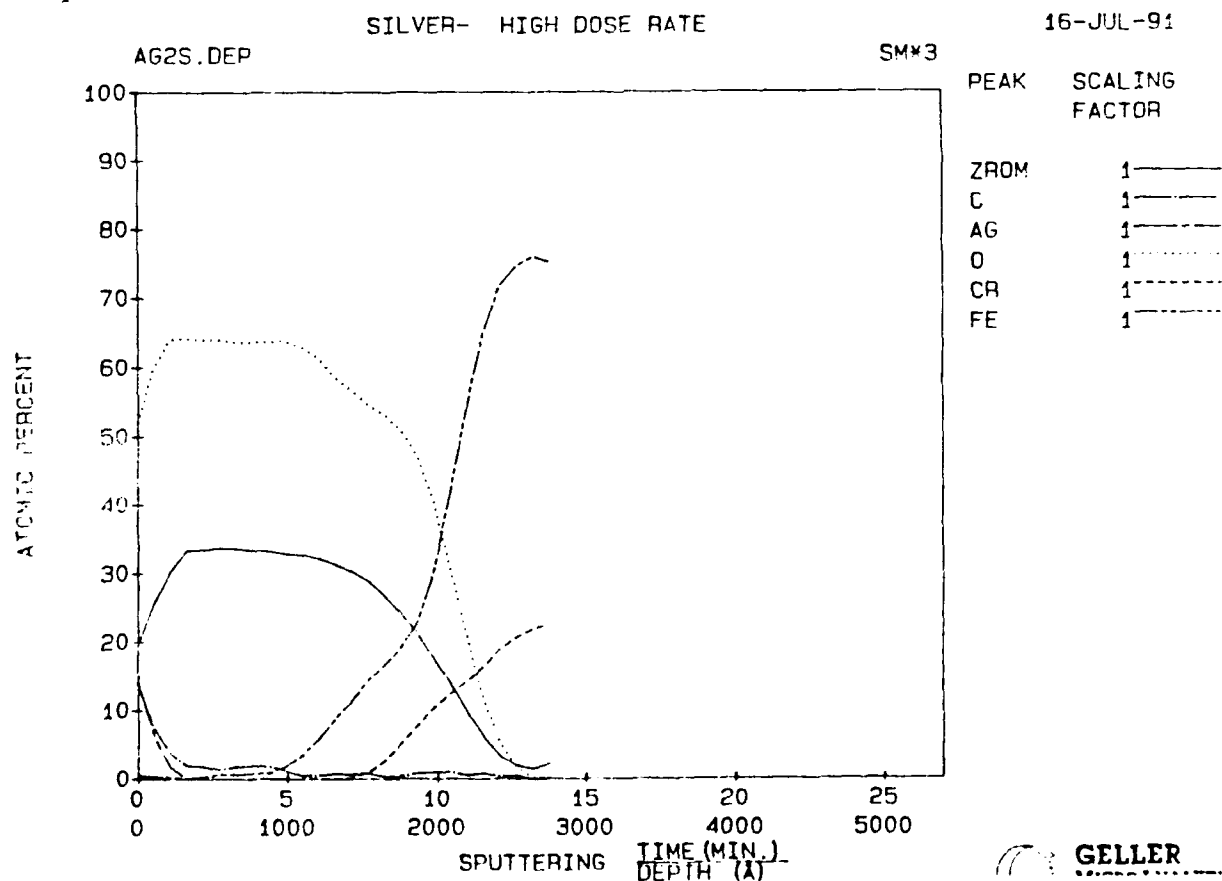


Figure 10. AES Depth Profile for the Primary Elements Found in the Sample.

Another surface contaminant, the Carbon, is harder to understand. Here, it is felt that the high value of 15 atomic % is probably due to incomplete cleaning of the sample and the solvents employed at the AES lab. Small quantities (less than 3%) of carbon were recorded in depth, and it is not clear if this is real or a statistical variation.

The Zirconium/Oxygen maintain the proper 1:2 stoichiometric ratio throughout for ZrO_2 , and this is very significant. An unusual feature, seen on more than one profile, is that the Iron component of the substrate rises at a significantly shallower depth than the Chromium component. The Oxygen profile also loses its 1:2 ratio to zirconium in this transition region with excess Oxygen present. It is presumed that the presence of pure Iron on the surface is responsible for the extra Oxygen. No control sample was analyzed, so it is not known whether the segregation of the Iron and Chromium was beam induced or inherent in the sample. We suspect it was beam induced, because our standard procedure was to sputter clean the substrate using the Zirconium beam for 10 minutes before starting the evaporation of the sacrificial coating. Differential sputtering effects could be occurring.

Characteristic of the ion implanted coating, there is no sharp interface, and the transition between substrate and Zirconia is gradual. This should have an important impact on improving adhesion.

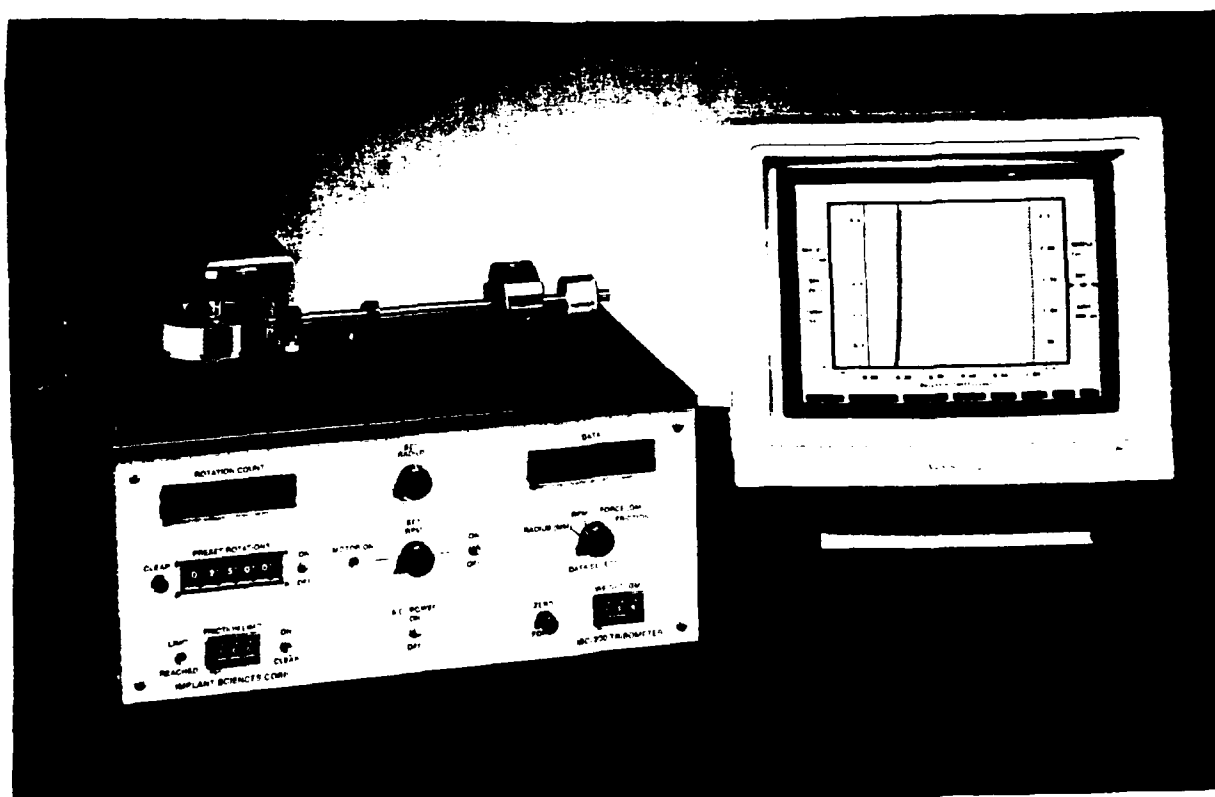


Figure 11. ISC-200 Tribometer

Adhesion-Scratch Test

We have used a modified version of our ISC-200 tribometer shown in Figure 11 to do a diamond scratch analysis for adhesion. In this test a diamond was drawn across the coating using a sequence of loads. For the heavier loads a hanging weight was used, and the load at the indenter was verified by measurement with a triple beam balance. For the lightest loads, the system counterweight were adjusted to select the load.

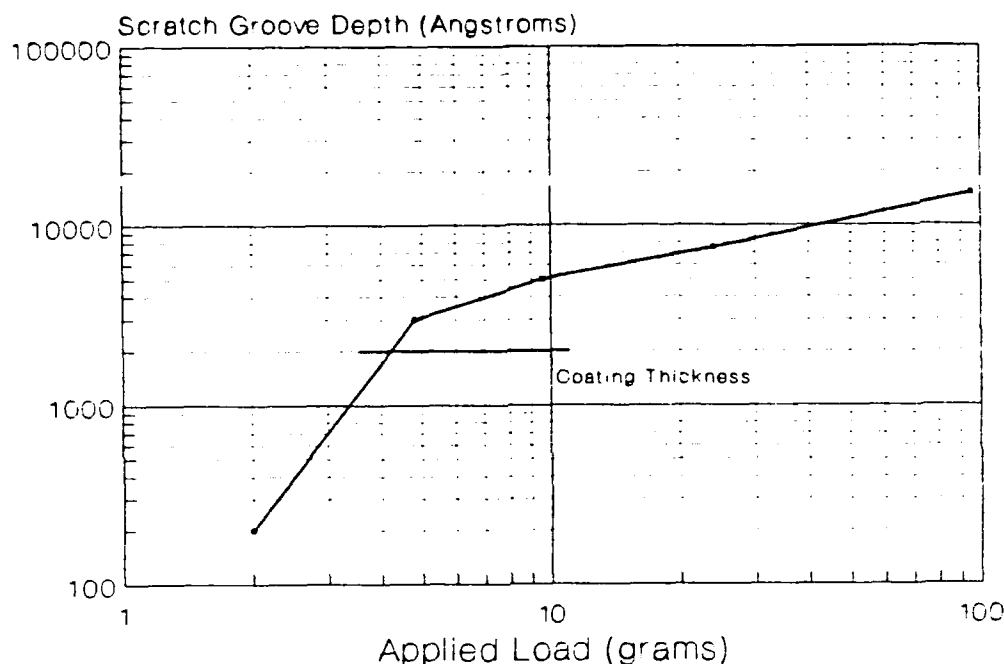


Figure 12. Groove Depth Versus Load on Diamond Indentor Scratch Test.

The groove depth versus load is shown in Figure 12. It can be seen that the coating was breached between 2 and 4.8 grams for this particular indenter. Visual observation, as shown in Figure 13 (2 grams) and 14 (4.8 grams) verifies this. The resultant groove has sharp edges and does not show signs of brittle fracture or delamination around the edges. The ceramic ZrO_2 coating appears to exhibit a ductile nature in Figure 13, and this has sometimes been observed with other types of ion assisted deposition processes. This has usually been attributed to the "nanodispersed" nature of the deposition process, which prevents large grains from growing.

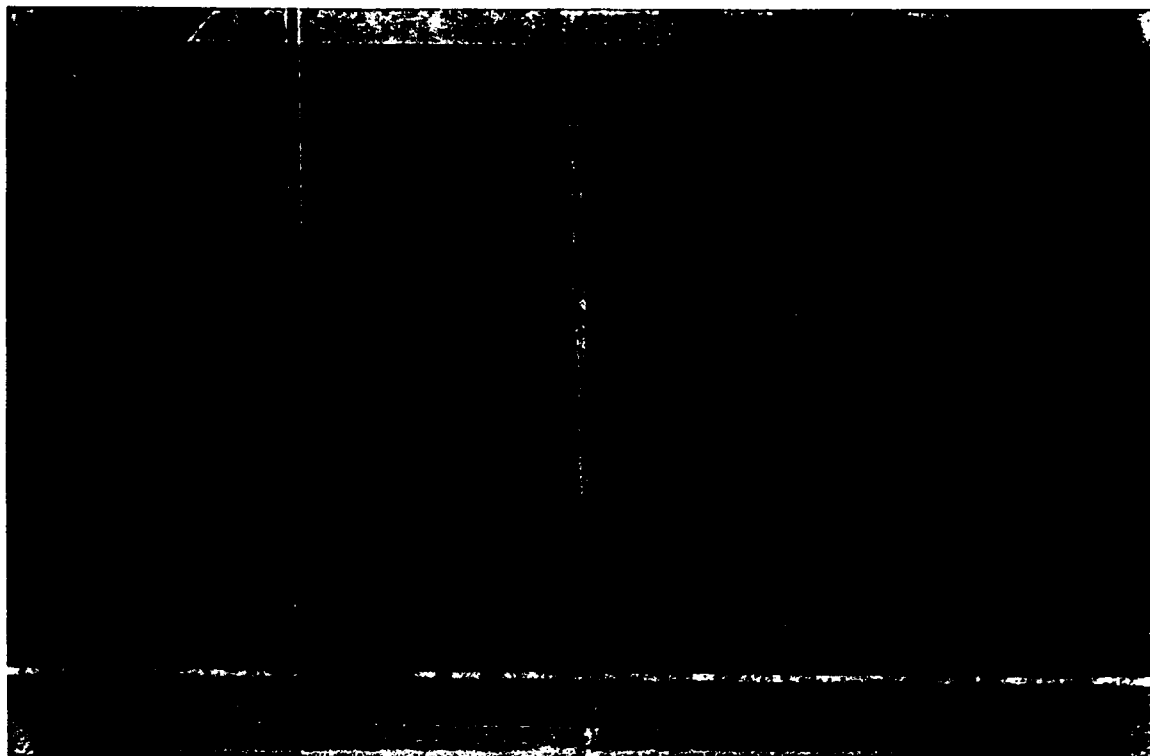


Figure 13. Photomicrograph of the Scratch Groove Created By the Diamond Indenter With an Applied Load of 2 Grams. The coating is not penetrated.

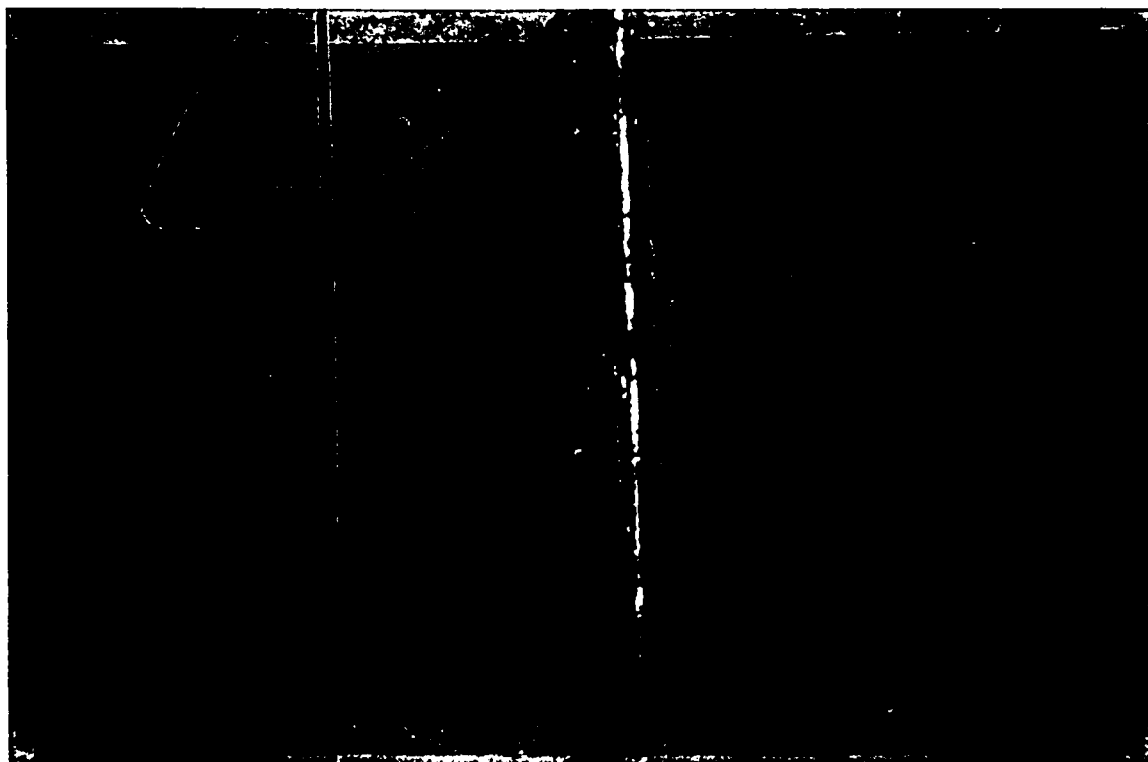


Figure 14. Same As Figure 3 But for 4.8 Grams.

Electrical Resistivity

Pure ZrO_2 should exhibit high electrical resistivity. The presence of small quantities of surface silver seen in AES may affect such a measurement unpredictably, however. A measurement indicated locally variable resistance, typically between 100K ohms and 1000K ohms. This suggests that a high resistance is likely, but not definitely confirmed.

Wear and Friction

The ISC-200 tribometer was used to perform a pin-on-disk wear test using a 7/16 inch diameter 440C ball as the pin. A load of 25 grams was applied, yielding a Hertzian pressure of 0.165 GPa and a contact diameter of 43.5 microns. The pin elastic modulus was 210 GPa and for ZrO_2 , a modulus of 156 GPa was used. The ball Poisson ratio was 0.3, and the disk was 0.324. The linear speed was 0.5 cm/second between pin and disk.

Figure 15 shows the friction as a function of the sliding distance. No lubricant was used. The starting value of friction was around 0.2, but a cyclical oscillation quickly developed. The run was stopped after about 1 meter of distance. Figure 16 shows the surface of the ZrO_2 disk after the test. Large amounts of adherent debris were being transferred from the pin. The oscillatory increase in friction occurred as the pin traversed these platelet of like material. The coating of ZrO_2 does not appear to have been eroded during the test, and only minor groove depressions are visible. A profilometer scan of the debris is shown in Figure 17 which confirms that material is being transferred to the ZrO_2 disk.

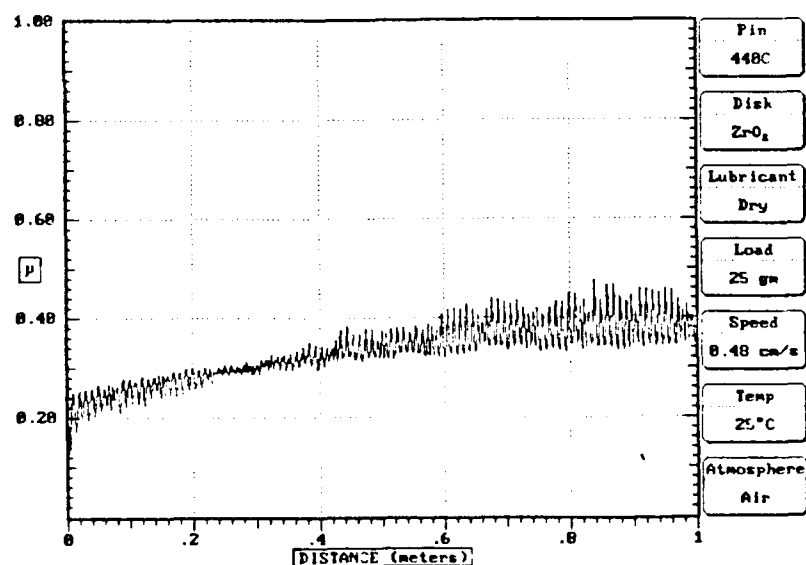


Figure 15. Friction Between 440C Pin and ZrO_2 Disk As a Function of Sliding Distance. The oscillations are probably caused by adhering pin debris on the disk.

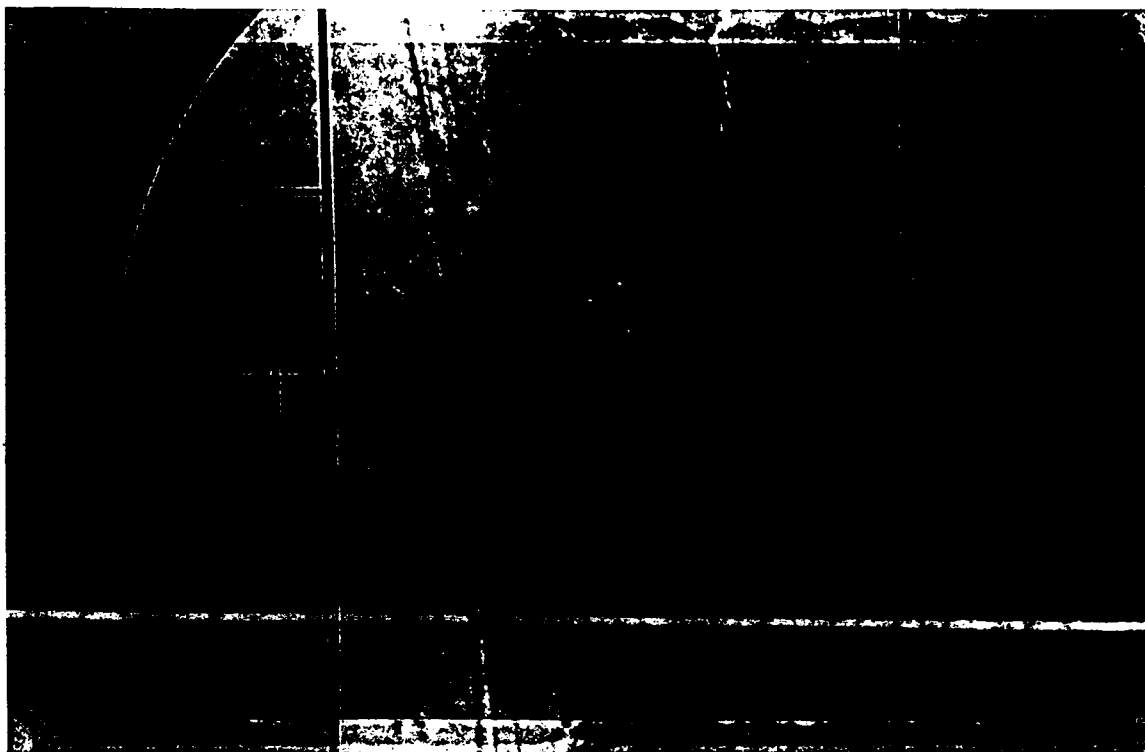


Figure 16. Photomicrograph of the ZrO_2 Disk at 500x After 1 Meter Sliding Distance. The material appears to be adhering pin debris.

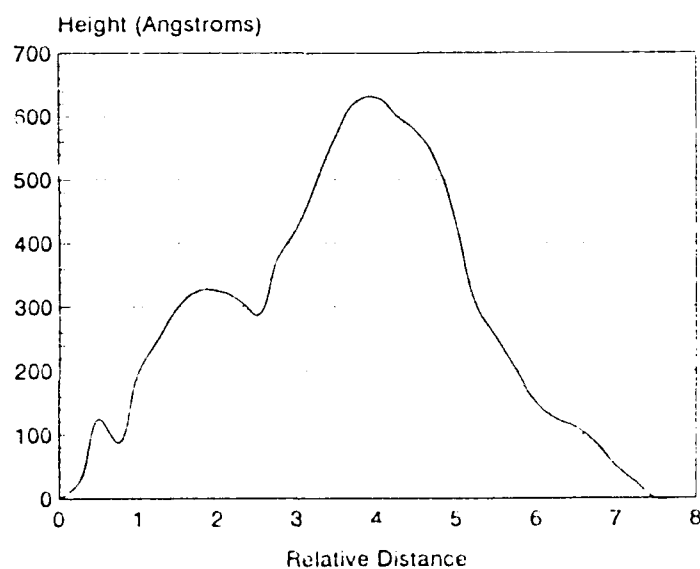


Figure 17. Profilometer Scan of the Debris Shown in Figure 16. The material is observed to be raised above the surrounding surface, indicating that material has been transferred to the disk.

Microhardness

A LECO MV-400 microhardness tester was used to characterize the ZrO_2 coating. The expected hardness is 1200 Knoop. Figure 18 shows the average measured values as a function of the applied indenter load. At high loads the hardness of the 316 SS substrate dominates the measurement. At low loads, the ZrO_2 dominates because the diamond indenter does not penetrate the coating. At a 2 gram load a microhardness similar to the expected value was observed. The error bars in the figure represent the standard deviation of at least 5 measurements at each load.

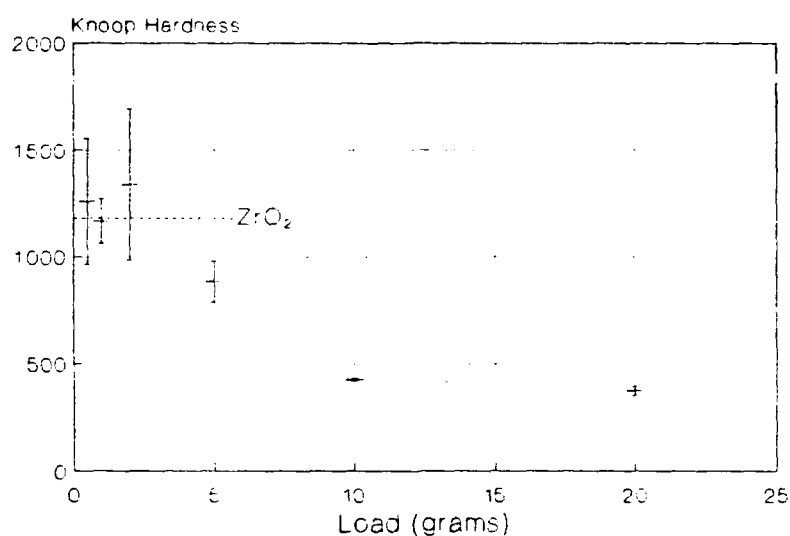


Figure 18. Microhardness Measurements on the ZrO_2 Coating with Variable Load. At 2 grams and below the measured value is probably due to the ZrO_2 coating rather than the substrate.

Thermal Stress

The sample was heated in air to 400°C and then rapidly quenched in LN_2 . No delamination of the coating was observed. This is a 600°C temperature range.

In summary, these tests have demonstrated the following results.

1. Stoichiometric ZrO_2 coating on steel is possible by ion beam coating.
3. The ZrO_2 contains no unexpected impurities and is optically transparent.
4. The coating is hard enough to resist wear in pin-on-disk testing with a bearing steel pin.

2.8 Cylindrical Samples

The use of ion beam coating would be very limited if only flat samples could be processed. A run was performed using a cylindrical M50 inner bearing race that was nominally 1 1/4 inches in diameter by 1/2 inch high. A groove for the raceway had a circular cross section extending $\pm 60^\circ$ from normal to the curved surface. Thus, a variety of angles was represented with this "complex" shape.

The sample was originally intended to be submitted to Cummins Engine Company for their analysis. However, it was decided that Cummins would prefer the treatment of a specific component of their diesel engine that was experiencing wear and corrosion problems. This component will be discussed in the next subsection.

Two M50 races were processed along with test coupons made from D2 tool steel. When it became clear that the M50 rings were no longer required, we decided to use the samples to test whether it would be feasible to build up a thicker coating of ZrO_2 by adding material using a conventional PVD process on the ion coated base.

The coating process followed the standard procedure listed below:

Ion - Zr^+ @ 150keV
Sacrificial coating - Silver
Dose - Nominally $2 \times 10^{18}/\text{cm}^2$
Pre-dose - Nominally $3 \times 10^{17}/\text{cm}^2$
Temperature - Cooled
Background - 2×10^{-5} Torr O_2
Samples - M50 Race and D2 Steel disk

The run was used to learn about any problems involving curved surfaces as well as study the effects of using ion beam sputtered ZrO_2 to further thicken the material. The results of the preliminary analyses are as follows:

Auger Spectroscopy

The D2 coupons were ion coated on their curved edge similar to the M50 races. The AES analyses occurred prior to adding a sputtered ZrO_2 layer nominally 3000Å thick. Figure 19 shows the observed results.

It is clear that the thickness of stoichiometric ZrO_2 (about 1200Å) is less than expected. The sample was continuously in the ion beam, and the sputtering coefficient was variable depending on the angle of incidence. Although the evaporation rate of the sacrificial layer was increased by 50% to accommodate this expected effect, it appears that the rate was still insufficient to fully compensate for the actual mean sputtering rate. This can be corrected easily by further increasing the rate of evaporation and is not a significant problem with the technique.

Figure 20 shows the estimated angular distribution of the sputtering coefficient for 150keV Zirconium implanted into Silver. Since the target was cylindrical, the incident current density is proportional to the cosine of the local incident angle. Thus, the second curve shows the sputtering coefficient corrected by this factor, which yields an effective coefficient which conveniently is nearly constant with angle. However, it is now suspected that the oversight which resulted in insufficient evaporant was the failure to include the effect of multiple incident angles from the evaporator. While the loss of atoms was essentially uniform over the illuminated area, the addition of sacrificial evaporant atoms was not. This lesson means that one must balance the mean flux of evaporant, taking into account the cosine effect.

Sputtered ZrO_2 Coating

An important test is to determine whether additional ZrO_2 can be added to the interface created by ion implantation. Many applications of ZrO_2 coatings require very thick layers which are beyond the capability of the implantation technique. A goal of this program has been to create an adherent bond coating, which then can act as a "primer" for conventional coating technologies.

Our initial trial has been to ion beam sputter additional ZrO_2 on the cylindrical M50 races. The process has been to sputter Zr in an oxygen ambient of 2×10^{-5} Torr. An intense directed Xe ion beam at 100keV was used on a Zr target. The final coating thickness was determined by means of Silicon witness plates which could be measured using a Tencor profilometer. One micron of ZrO_2 was found to be added, and although we have not analyzed the material, the visible color fringes suggest that the deposit is ZrO_2 and not Zr.

Bonding to the substrate appears to be good. A preliminary, uncontrolled scratch test with a diamond scribe indicated no brittle fracture or delamination of the added coating. Multiple Thermal cycling between +300°C and -194°C (total=500°C) showed no evidence of delamination after 10 cycles.

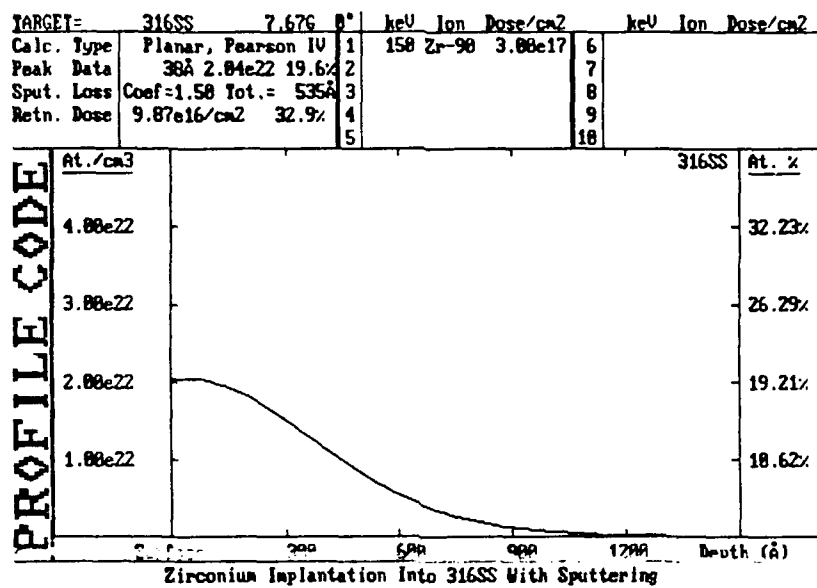


Figure 19. Auger Analysis of the ZrO₂ Implanted Sample

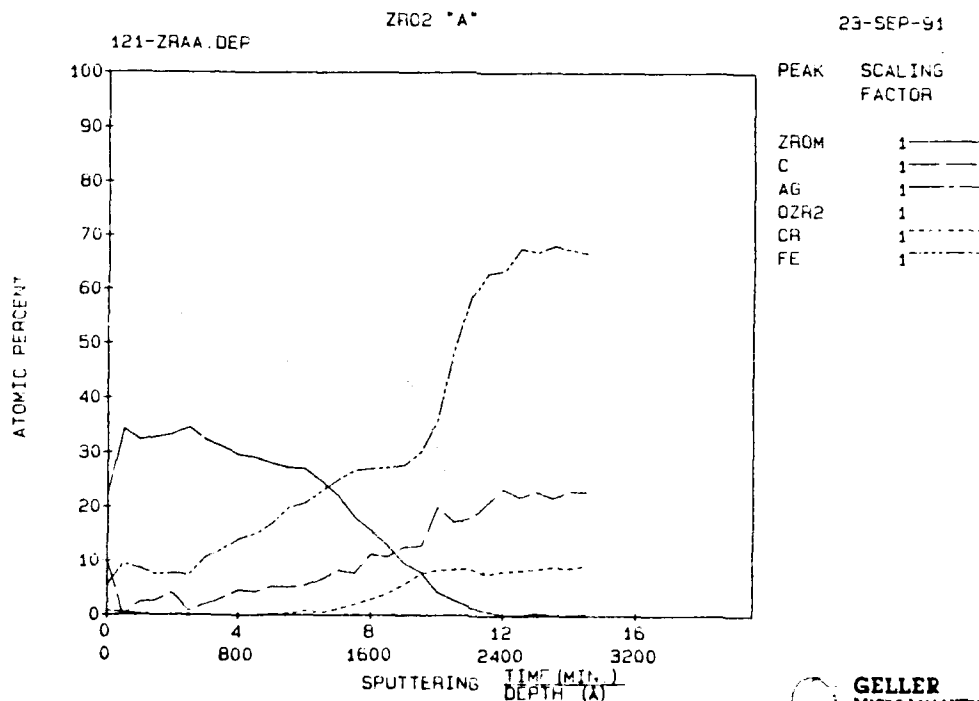


Figure 20. Predicted Sputtering Coefficient and Loss of Atoms for a Cylindrical Sample Using 150keV, Zr⁺ into Silver